Universities Council on Water Resources
Journal of Contemporary Water Research & Education
Issue 168, Pages 106-118, December 2019

Investigating Relationship Between Soil Moisture and Precipitation Globally Using Remote Sensing Observations

Robin Sehler[1], *Jingjing Li[1], JT Reager[2], and Hengchun Ye[3]

*[1]Department of Geosciences and Environment, California State University, Los Angeles; [2]Jet Propulsion Laboratory; [3]College of Natural and Social Sciences, California State University, Los Angeles; *Corresponding Author*

Abstract: The complex relationship between precipitation and soil moisture plays a critical role in land surface hydrology. Traditionally, the analysis of this relationship is restricted by the spatial coverage of both soil moisture and precipitation data that are collected through in-situ observations at limited locations. In this study, we utilized the National Aeronautics and Space Administration (NASA)'s remote sensing products of soil moisture (SMAP: Soil Moisture Active Passive) and precipitation (TRMM: Tropical Rainfall Measuring Mission), which provide near-global coverage, to investigate the co-variation of precipitation and soil moisture regionally, as a function of ecosystem types and climate regimes. We apply information on land cover and climate regimes to provide insight about correlation strength of soil moisture and precipitation. The results indicate that most of the globe has a moderate to strong positive correlation of SMAP soil moisture and TRMM precipitation data during the study period. In relation to land cover, soil moisture and precipitation have the strongest correlations in regions of limited vegetation, whereas forests and densely vegetated regions have weaker correlations. As for climate regimes, they have the strongest correlations in arid or cold regions, and weaker correlations in humid, temperate locations. While remotely sensed soil moisture data are less reliable in dense vegetation, these results confirm that drier, less vegetated climates show a highly linear relationship between soil moisture and rainfall.

Keywords: *TRMM precipitation, SMAP soil moisture, global relationship, satellite observations*

Surface soil moisture accounts for an estimated 0.001% of the volume of Earth's freshwater, and yet, this tiny layer of water plays a powerful role in the hydrologic cycle (McColl et al. 2017). The amount of water in the top soil influences how much heat is exchanged between the land and the atmosphere, along with important hydrologic processes, such as precipitation, river discharge, flood, and drought. Due to its influence, soil moisture is used to forecast weather, predict climate change, estimate agricultural yields, and provide early warning for flood and drought (Entekhabi et al. 2010).

The interplay of precipitation and soil moisture strongly affects the terrestrial water and energy cycles. Some aspects of this relationship are straight-forward, while others are controversial. The spatial and temporal patterns of soil moisture depend on the variability of precipitation, evapotranspiration, and runoff (Famiglietti and Rodell 2013; McCabe and Wolock 2013). However, there are more uncertainties regarding soil moisture's role as a feedback mechanism for precipitation and other hydrologic components than its dependence on above-mentioned hydrologic components (Koster et al. 2004; James and Roulet 2009; Liang et al. 2010).

The interaction between soil moisture and precipitation is complex, varying regionally in correlation direction (i.e., positive/negative) and magnitude (i.e., weak/strong). Previous research has identified some physical mechanisms causing

positive correlations between soil moisture and precipitation (Findell and Eltahir 1997; Eltahir 1998; Zheng and Eltahir 1998). These studies support the hypothesis that wetter soil can provide abundant moisture to the atmosphere, increasing humidity and, as a result, enhancing precipitation. From the energy-balance point of view, wetter soil decreases the surface albedo that allows for an increase in net solar and terrestrial radiation, and an increase in moisture convergence, which may ultimately enhance the precipitation. Such a mechanism supports the well-known hypothesis, "wet regions get wetter, dry regions get drier," which theorizes higher risks of floods in wet regions and higher risks of droughts in dry areas.

However, recent studies suggest that in certain localities, soil moisture and precipitation are negatively correlated (Cook et al. 2006; Guillod et al. 2015; Yang et al. 2018). For example, more precipitation is observed in dry soil regions such as Southern Africa because of the strengthened convective system (Cook et al. 2006), which indicates an increase in the risk of floods in dry areas. This opposite phenomenon challenges the well-known "wet regions get wetter, dry regions get drier" trend (Greve et al. 2014; Feng and Zhang 2015) and creates controversy about the soil moisture-precipitation relationship. Moreover, the soil moisture and precipitation interaction is strongly affected by the local climate and environment (Boé 2013; Ford et al. 2015a; Ford et al. 2015b). These bodies of research imply that environmental factors, such as land cover and climate regimes, may play a significant role in how soil moisture interacts with precipitation.

In addition to environmental factors, the study of soil moisture and precipitation is further complicated by the availability and quality of the data. The technology of soil moisture measurements has dramatically advanced in recent years. They are no longer limited to sparse networks of in-situ samplings but have near-global coverage through remote sensing. The Satellite era soil moisture datasets include Advanced Microwave Scanning Radiometer - Earth Observing System (AMSR-E) (Wentz et al. 2014), Soil Moisture and Ocean Salinity (SMOS) (Kerr et al. 2013), and Soil Moisture Active Passive (SMAP) (O'Neill et al. 2016). Although these datasets represent great technological advances in the study of soil moisture, they require validation to ensure data quality.

Launched in 2015, SMAP is the newest satellite soil moisture dataset. Like its predecessor SMOS, SMAP has an L-band radiometer, ideal for detecting soil moisture through layers of vegetation. The initial science objective of the SMAP mission was to provide unprecedented, high-resolution global soil moisture data from the combination of the active and passive sensors. Unfortunately, the power source of SMAP's active radar lost functionality months after its deployment. Thankfully, data from SMAP's passive radiometer were salvaged, albeit at a coarser resolution. As a newer dataset, and in light of the technical challenges that befell the SMAP mission, validation of SMAP data is necessary to understand if the mission was still successful in producing valuable soil moisture data, after losing its most important sensor.

SMAP was considered a better dataset than AMSR2, when compared with in-situ soil moisture samples across the Great Plains (Zhang et al. 2017). SMAP also outranked seven other satellite soil moisture datasets, in comparison to in-situ soil moisture data, over the Little Washita Watershed Network (Cui et al. 2018). Additionally, SMAP products have been validated against one another, including the data produced from the active sensor, from the passive sensor, and from the combination of the active and passive sensor. In a validation study over Northwestern China, SMAP's passive sensor's soil moisture dataset fared better than datasets from the active sensor, and all three datasets were shown to estimate soil moisture better over bare soils than over soils with vegetation (Ma et al. 2017).

The goal of this study is to assess the relationship between soil moisture and precipitation at a global scale using SMAP soil moisture measurements and Tropical Rainfall Measuring Mission (TRMM) precipitation estimates, and to investigate how such a relationship varies with different land cover type and climate regime. It is worth noting that this is the first attempt to relate SMAP soil moisture data to TRMM precipitation data over a global coverage. This study also explores the possibility of using TRMM precipitation data to validate SMAP soil moisture data. TRMM is a well-respected dataset

in the satellite precipitation community (Sapiano and Arkin 2009). In theory, the SMAP data will clearly reflect increased soil moisture levels over regions where the TRMM satellite indicates precipitation. Because the expected relationship between precipitation and soil moisture is strong, precipitation would be used to informally validate the accuracy of soil moisture data. Strong correlations between the TRMM precipitation and SMAP soil moisture datasets could be interpreted as indication of SMAP's accurately estimating global soil moisture levels. However, it is also understood that many factors, such as land cover and climate, influence the infiltration of rain water into soil.

Data

Soil moisture data come from the SMAP satellite, available through the National Snow and Ice Data Center (NSIDC) (https://nsidc.org/data/SPL3SMP/versions/4). Despite losing the functionality of its active microwave radar, soil moisture estimates using SMAP's passive microwave radiometer have proven to outperform other satellite soil moisture datasets when compared to in-situ soil moisture data (Ma et al. 2017; Cui et al. 2018). SMAP's microwave radiometer senses the thermal heat radiating from the surface of the earth, and the intensity of heat sensed is proportional to the product of the thermal emissivity and brightness temperature. The soil moisture measurements were estimated using the Tau-Omega model and brightness temperatures (Das et al. 2015). SMAP's sensor measures the near-surface soil moisture (0-5 cm depth) in cm^3/cm^3. The Level 3, Version 4 dataset used in this study comes from SMAP's passive microwave radiometer providing daily coverage from March 31, 2015 (O'Neill et al. 2016). However, near-global coverage is only available every three days (Entekhabi et al. 2014). The data's nominal spatial resolution is 36 km by 36 km, based on the Equal-Area Scalable Earth Grid (EASE-Grid) 2.0 (Brodzik et al. 2012). Global spatial coverage is limited to Latitudes 85.044° to -85.044° and Longitudes -180° to 180°. Additionally, SMAP Level 3 retrievals are bound to vegetation and ice thresholds. SMAP Level 3 data contain vegetation flags for any grid cell with a vegetative water content greater than 5 kg/m^2. SMAP Level 3 data also have a frozen soil flag which assesses the frozen soil area fraction. When the frozen soil area fraction is greater than 0.5, a flag is set and soil moisture is not retrieved (O'Neill et al. 2018). Because of SMAP's vegetation and ice flags, soil moisture data are unavailable in certain regions of the Amazon Rainforest and in some higher latitude locations.

Precipitation data come from the TRMM satellite, available through the NASA Goddard Earth Sciences (GES) Data and Information Center (DISC) (https://disc.gsfc.nasa.gov/datasets/TRMM_3B42_Daily_V7/summary). TRMM collected data through its passive microwave sensor and precipitation radar. This study utilizes the 3B42 Version 7 Research Derived Daily Product dataset (Huffman and Bolvin 2015). The spatial resolution of the data is 0.25° by 0.25° with the near-global coverage of Latitudes 50° to -50° and Longitudes -180° to 180°. This dataset is based on the Version 7 TRMM Multi-Satellite Precipitation Analysis (TMPA) algorithm, which consists of passive microwave derived precipitation estimates and microwave-calibrated infrared precipitation estimates filling in the gaps of microwave imageries, corrected by ground-based gauges (Huffman et al. 2007).

The Moderate Resolution Imaging Spectroradiometer (MODIS) instrument on NASA's Terra and Aqua satellites, provides land cover classifications through the University of Maryland's Global Land Cover Facility. This study uses the MCD12Q1, Version 5.1 dataset, specifically the most recent 2012 classification (Channan et al. 2014). The classification includes 17 land cover types with 0.5° by 0.5° spatial resolution. Latitudinal coverage spans -64° to 84° and longitudinal coverage spans -180° to 180°.

The Köppen-Geiger climate classification (Peel et al. 2007) was obtained through NASA's Oak Ridge National Laboratory (ORNL) Distributed Active Archive Center (DAAC) (https://webmap.ornl.gov/ogc/dataset.jsp?ds_id=10012). This dataset categorizes the globe by climate, considering average temperature and precipitation trends. The classification scheme identifies five main climates, six categories of precipitation, and seven categories of temperature. The spatial

resolution is 0.5° by 0.5° with latitudinal coverage spanning -90° to 90° and longitudinal coverage spanning -180° to 180°.

Methodology

In order to assess the relationship of precipitation and soil moisture, the two datasets were preprocessed to have the same spatial coverage and uniform grid resolution. Through examining the SMAP soil moisture estimates, it showed that the 8-day composites of the soil moisture were able to provide optimal global coverage, while the suggested 3-day composites (Entekhabi et al. 2014) still have spatial gaps. Thus, the 8-day composites of SMAP soil moisture were created, which contain the average soil moisture estimate from the samples within that period. Composites using the least number of days were preferred over monthly composites, for example, in order to highlight the more immediate interactions between precipitation events and soil moisture, as close in time to the events as possible. Likewise, 8-day composited averages were created for the TMPA precipitation data. The study period is from March 31, 2015 to June 23, 2016. Three SMAP daily estimates were unavailable (May 13, 2015, December 16, 2015, and May 1, 2016). In total, 448 daily files were compiled into 56 8-day composites for each dataset over the study period. Next, SMAP soil moisture's composites were subset to the TMPA's spatial coverage. In order to obtain uniform grid resolution between the datasets, TMPA's grid resolution of 0.25° by 0.25° was linearly interpolated to SMAP's EASE-Grid 2.0 nominal resolution of 0.36° by 0.36°. Such linear interpolation is a common technique of matching datasets spatial resolutions for further analysis in the hydrology community (e.g., AghaKouchak et al. 2011; Pan et al. 2019).

Finally, TMPA data were correlated to SMAP data, using MATLAB's "corrcoef" function. The formula used in "corrcoef" function to compute Pearson's Correlation Coefficient is shown below (Fisher 1958):

$$\rho(T,S) = \frac{1}{N-1}\sum_{i=0}^{N}(T_i-\mu_T)(S_i-\mu_S)\left(\frac{1}{\sigma_T}\right)\left(\frac{1}{\sigma_S}\right)$$

Where, ρ is the correlation coefficient between TMPA precipitation (T) and SMAP soil moisture values (S) per grid cell; N is the total number of grid cells; T_i is the precipitation value per grid cell; S_i is the soil moisture value per grid cell; μ_T is the mean of T; μ_S is the mean of S; and σ_T and σ_S are the standard deviations of T and S, respectively. Both Pearson's Correlation Coefficient and p-values indicating a confidence level of 95% were calculated for each grid location, except oceans and grids with missing data. After correlation coefficient values were calculated, significance tests (using p-values) were carried out to determine which coefficient values were statistically significant. The percentages of grids with statistically significant correlation values were calculated according to correlation strength. Three locations were selected for time series analysis, in order to display a region with a strong positive correlation value, an irrigated region, and a region with a negative correlation value.

To investigate how environmental factors affect soil moisture-precipitation interactions, results were spatially summarized according to land cover types and climate regimes. First, statistically significant correlation coefficient values were interpolated using linear interpolation to match MODIS Land Cover Classification grid resolution of 0.5° by 0.5°. Next, the land cover classification data were used to index correlation values according to their land cover type; the correlation values were spatially averaged, resulting in one average correlation value per land cover type. The same process was carried out for climate classification defined by the Köppen-Geiger climate classification, which results in one average correlation value per climate class.

Results

Figure 1 displays a sample 8-day composite obtained from TMPA daily products, spanning March 31, 2015 to April 7, 2015. Figure 2 displays a sample 8-day composite obtained from SMAP during the same period. These figures show the pattern that regions with the highest levels of precipitation (Figure 1) generally occur where regions experience the highest soil moisture levels (Figure 2). The strong relationship between these two figures indicates that elevated precipitation is generally associated with elevated soil moisture levels.

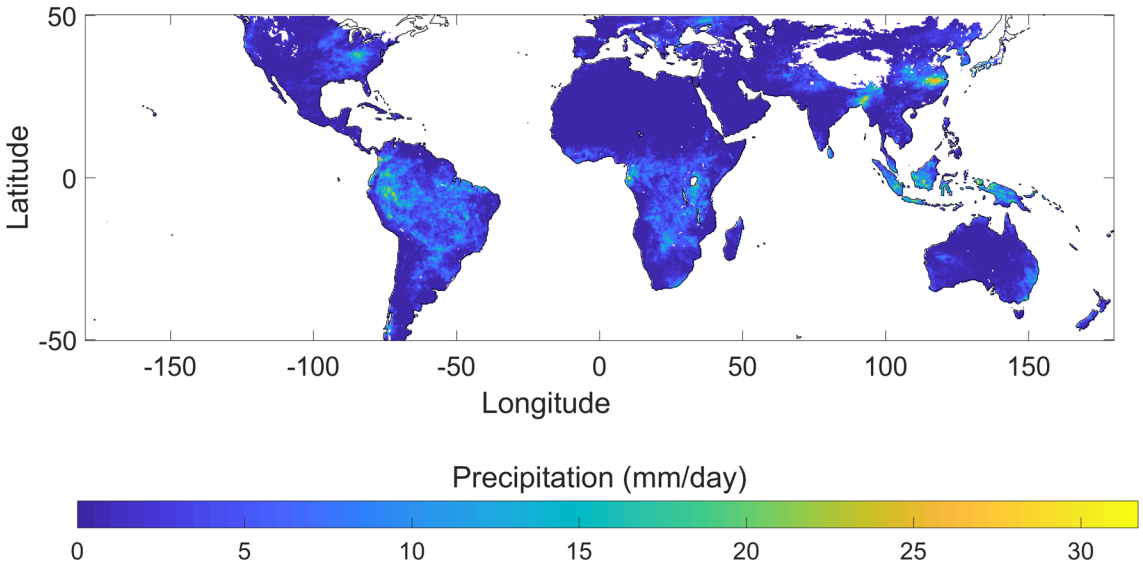

Figure 1. A sample 8-day composite of daily precipitation data obtained from TRMM 3B42 V7 from March 31, 2015 to April 7, 2015.

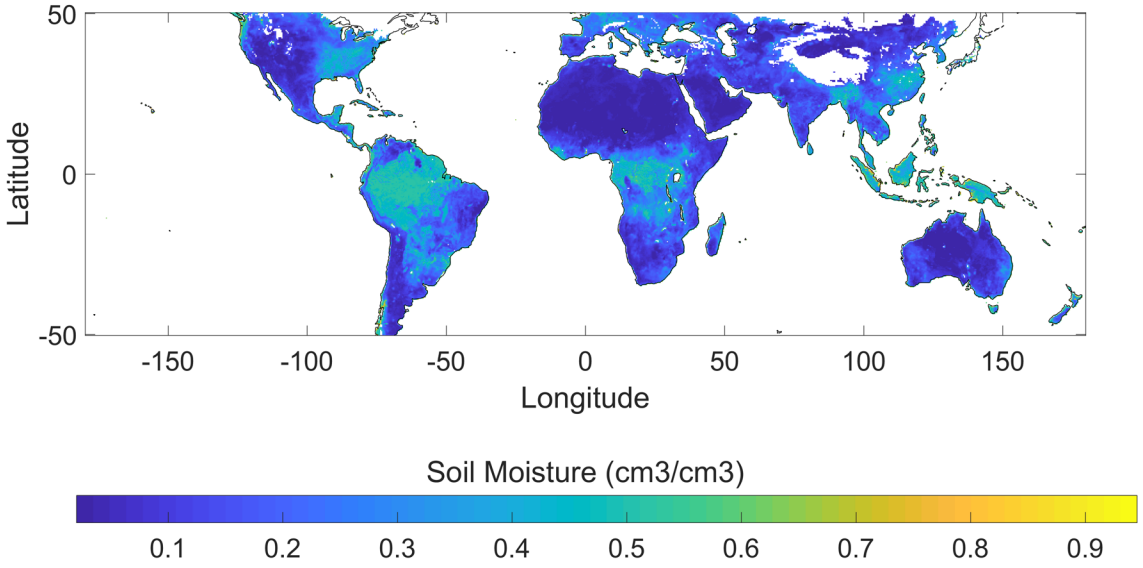

Figure 2. A sample 8-day composite of daily soil moisture data obtained from SMAP from March 31, 2015 to April 7, 2015.

Figure 3 displays Pearson's correlation coefficient for 8-day composites of the TMPA precipitation and SMAP soil moisture datasets in the study period. This figure shows a pattern of moderate to very strong positive correlations occurring in every continent. The strongest correlations occurred in Africa, Central America, the Middle East, Asia, Australia, the eastern portion of South America, and much of the Western United States. Moderate to weak correlations occurred in the Central and Eastern United States, Northern and Southern Africa, and north-east of the African Sahel. Additionally, moderate to weak correlations occurred throughout Europe, Southern Australia, Malaysia, Indonesia, and Papua New Guinea.

On the other hand, Figure 3 shows that the largest negatively correlated regions occurred in major river basins, such as the Amazon and Congo. This could be due to the physical process of hydraulic redistribution. Harper et al. (2010) documented that

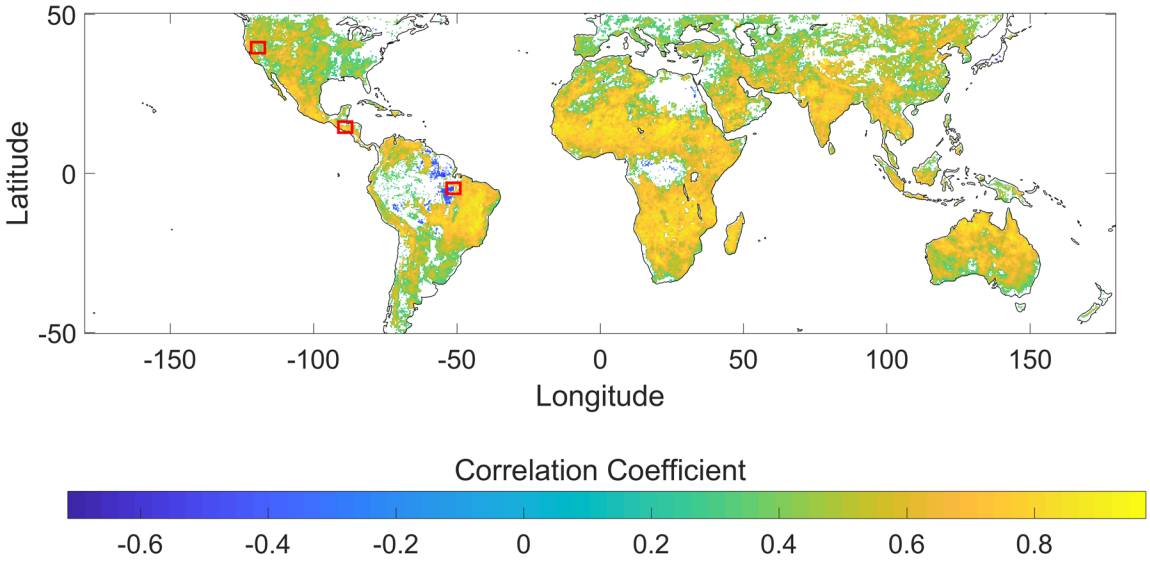

Figure 3. TMPA precipitation versus SMAP soil moisture correlation coefficients by grid cell with significant P values (< 0.05). 8-day composites spanning March 31, 2015 to June 23, 2016. The non-significant correlation coefficients are omitted and these grids are colored white. Red-colored rectangles located in Central America, Central California, and the Amazon Rainforest indicate time series locations for Figure 5.

Amazon trees with long roots perform hydraulic redistribution from deep to shallow soil, in order to survive dry seasons. Yan and Dickinson (2014) assert that a similar process occurs in the Congo River Basin, where deeply rooted trees perform hydraulic redistribution. In addition, non-positive correlations occur in Northeast Africa and Japan, and both coincide with river systems. The physical process of river transport creates conditions leading to an inverse relationship between precipitation and soil moisture: when precipitation occurs upstream, it would cause downstream portions of the river to expand, without downstream regions necessitating direct precipitation. Such is the case in Northeast Africa, where the Nile River is famous for its seasonal expansion. Heavy rains occur on the Nile River in Ethiopia and cause it to expand as it heads north into Egypt and Sudan (Conway 2000). Therefore, soil moisture along the Nile in Sudan and Egypt increases, independent of direct rainfall in Sudan and Egypt (Conway 2005).

Figure 4 displays the percentages of varying correlation strengths, which show that precipitation and soil moisture mostly correlate moderately to very strongly. 72.89% of the statistically significant grids displayed a moderate to very strong correlation, while 21.62% exhibited weak to very weak correlations. In addition to the prevalence of moderate to very strong correlations, the correlations are mostly positive, covering 93.07% of the globe, which is consistent with the previous literature (Findell and Eltahir 1997; Eltahir 1998; Zheng and Eltahir 1998). In these locations, as precipitation increases, soil moisture increases; or as precipitation decreases, soil moisture also decreases. The general trend of a moderate to strong correlation magnitude and a positive correlation direction supports the hypothesis that typically, precipitation leads to an increase in soil moisture. However, 1.44% of grids have negative correlations, indicating that soil moisture reacts to precipitation in an opposite way. Such negative relationships were observed by several other studies and were caused by different environmental and climatic factors (Cook et al. 2006; Guillod et al. 2015). For instance, Yang et al. (2018) specified that negative correlations occur in locations which have physical, limiting mechanisms such as having limited soil moisture, or being low in energy input.

One sample grid from each of the three locations, in Central America, Central California, and the Amazon Rainforest, was selected to show how SMAP soil moisture varies with TMPA precipitation for a region with a strong positive correlation, an irrigated region, and a region with

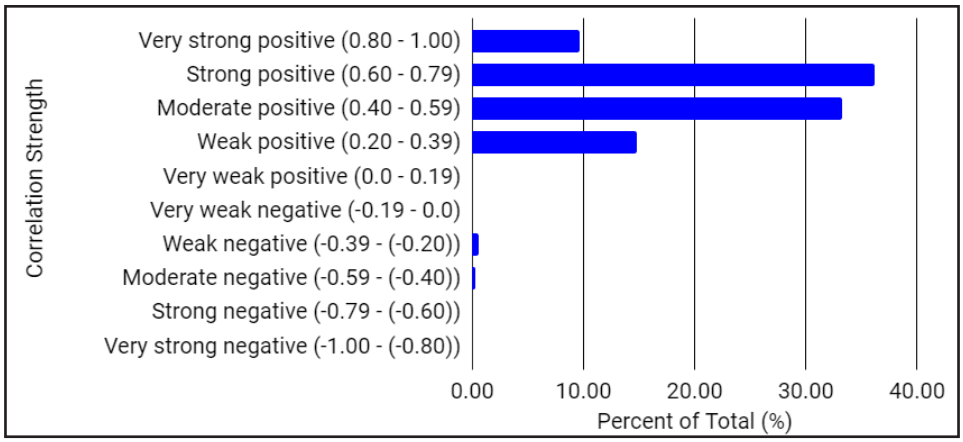

Figure 4. Bar plot of correlation strength by percent of total statistically significant grids.

a negative correlation, respectively. Figure 5a displays a time series of TMPA precipitation and SMAP soil moisture in Central America for the study period. This location represents a region where correlation coefficients are predominantly positive and moderately strong. The figure reveals a pattern that where precipitation rises soil moisture also rises. Figure 5b displays a time series in Central California, a heavily irrigated location. Patterns seen in the figure show that increases in precipitation coincide with increases in soil moisture, but increases in soil moisture also occur at times when precipitation does not occur. This dynamic is an expected scenario in the context of irrigation and watering of crop lands. Figure 5c displays a time series in the Amazon Rainforest, where concentrations of negative correlations occur. The figure reveals the pattern that soil moisture increases at times when precipitation is not present, which agrees with the findings from Harper et al. (2010) that top soil is moistened by groundwater during the dry season through the hydraulic redistribution process.

The average correlation coefficient by land cover type over the study period is shown in Figures 6 and 7 in order to understand how the precipitation and soil moisture relationship varies with the land cover. These figures reveal that precipitation and soil moisture are positively correlated under every type of land cover. The strongest positive correlations are found in land cover classes such as savannas, closed shrublands, woody savannas, mixtures of cropland and natural vegetation, open shrublands, and barren or sparsely vegetated. The land cover region showing the weakest positive correlation was permanent wetlands. These findings indicate that precipitation and soil moisture have the strongest correlations in regions of limited vegetation, whereas forests and densely vegetated regions have weaker correlations between precipitation and soil moisture. Figures 8 and 9 display the average correlation between TMPA precipitation and SMAP soil moisture, by Köppen-Geiger climate classification regimes. The same pattern was discovered as the land cover analysis, indicating that the precipitation and soil moisture correlation is positive across the climate regimes after averaging the correlation values per climate regime. These two figures reveal that South America, Africa, India, Australia, Central America, and parts of Europe have the highest correlation values. Also, precipitation and soil moisture have the strongest correlations in regions that are arid and dry or cold, and weaker correlations in humid, temperate locations.

Conclusion

This study assessed the relationship between precipitation and soil moisture using remotely sensed TRMM and SMAP measurements from March 31, 2015 to June 23, 2016. In order to calculate the correlation coefficients and their significances across the globe, 8-day composites of each dataset were created for coherent global coverage. Most grids showed a moderate to strong positive correlation between SMAP soil moisture and TMPA precipitation data. Precipitation and soil

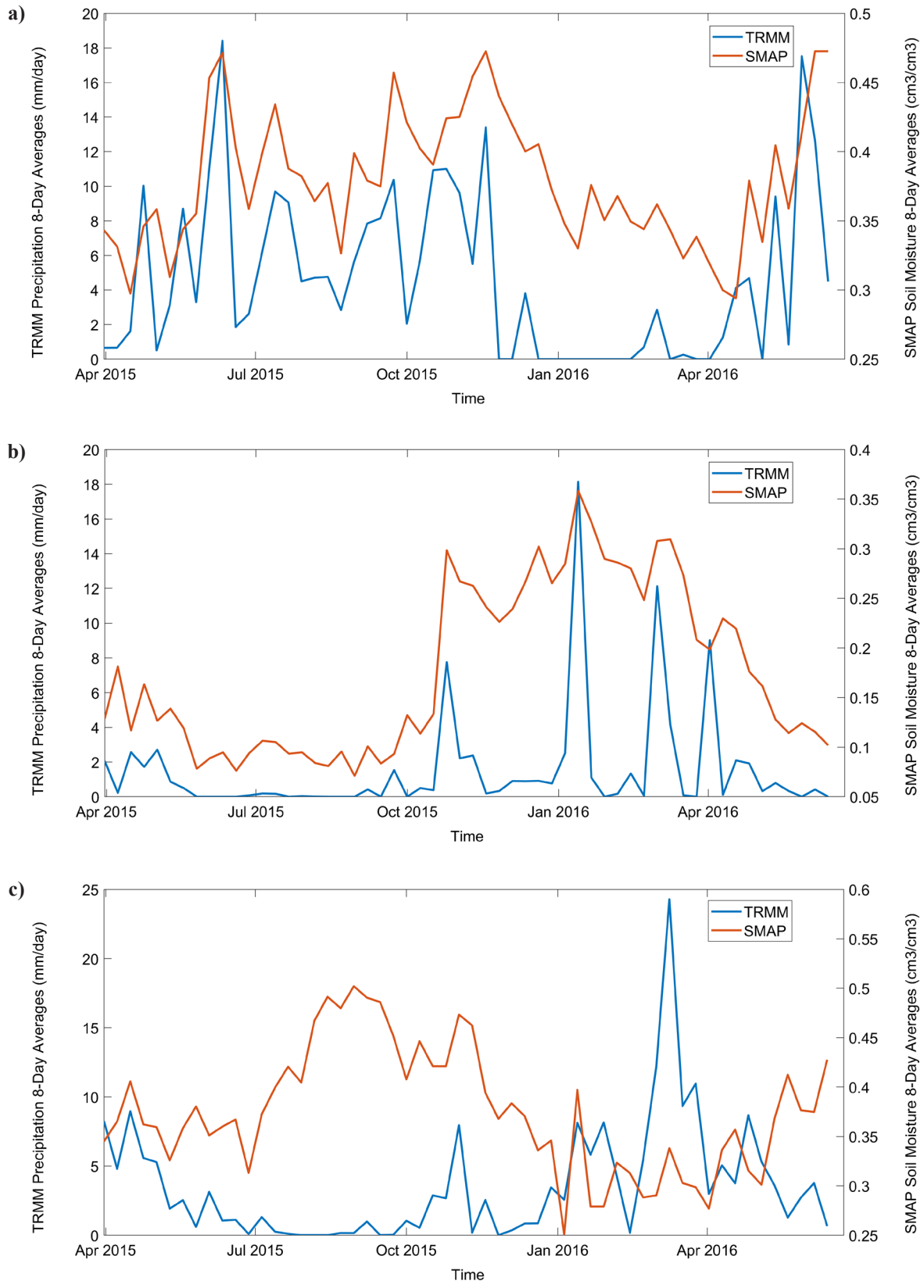

Figure 5. Time series for three locations in a) Central America, b) Central California, and c) Amazon Basin.

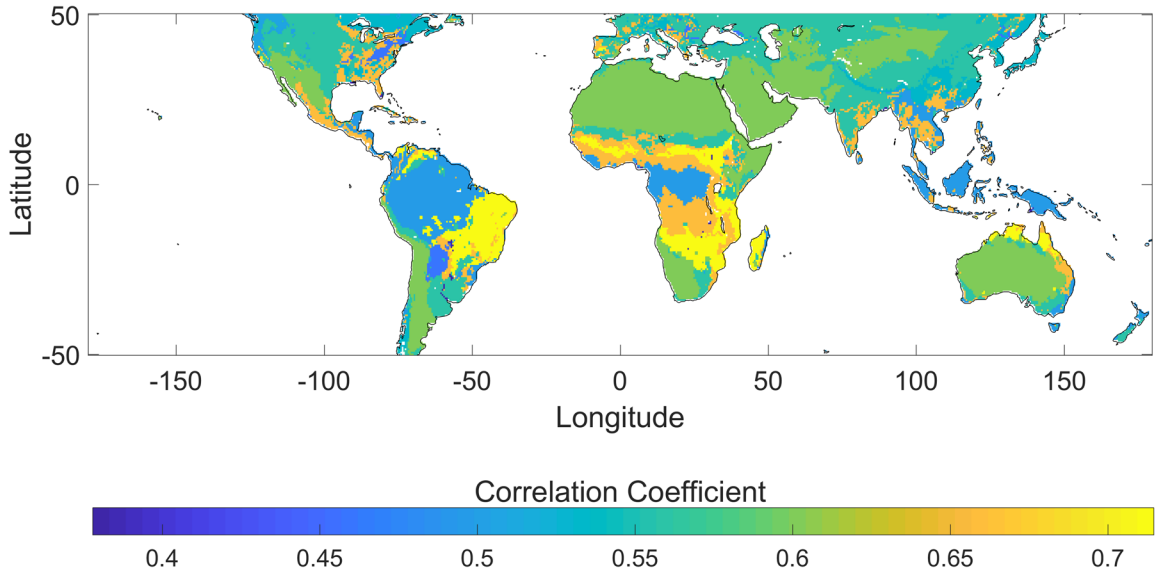

Figure 6. Average correlation coefficients by land cover type.

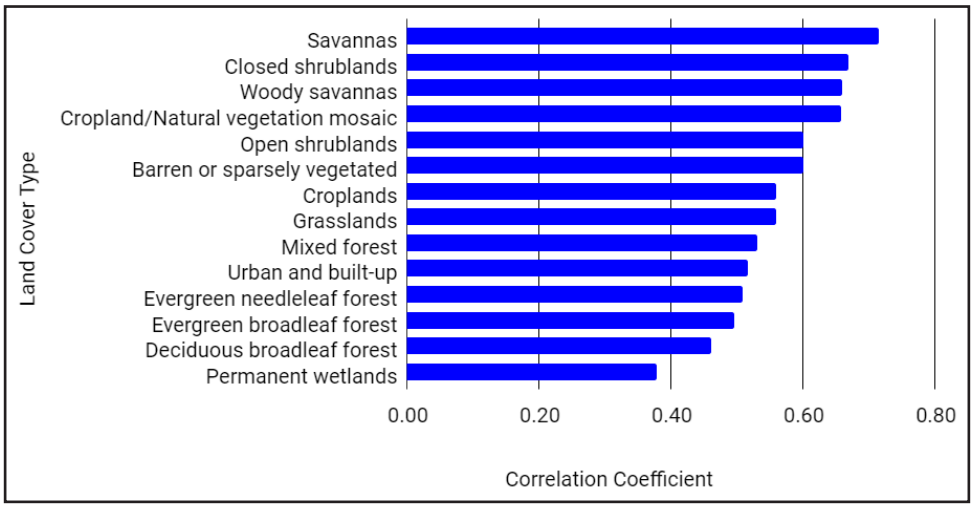

Figure 7. Bar plot of average correlation coefficient by land cover type.

moisture have the strongest correlations in regions of limited vegetation, whereas forests and densely vegetated regions have weaker correlations. Similarly, precipitation and soil moisture have the strongest correlations in regions that are arid and dry or cold, and weaker correlations in humid, temperate locations.

Overall, this study revealed that the relationship between precipitation and soil moisture goes deeper than what is seen on the surface. Although several other studies have revealed that negative correlations exist between precipitation and soil moisture (Cook et al. 2006; Guillod et al. 2015; Yang et al. 2018), the time series analysis conducted in this study reveals which of two mechanisms is causing negative correlations: either a) soil moisture increases while precipitation does not increase (i.e., decreases or stays the same) or b) soil moisture decreases while precipitation does not decrease (i.e., increases or stays the same). The time series helped explain that, specifically, in both the Amazon Rainforest and in Central California, soil moisture, at times, increased while precipitation did not increase. This study indicates that soil moisture and precipitation are not always positively correlated, and that the relationship

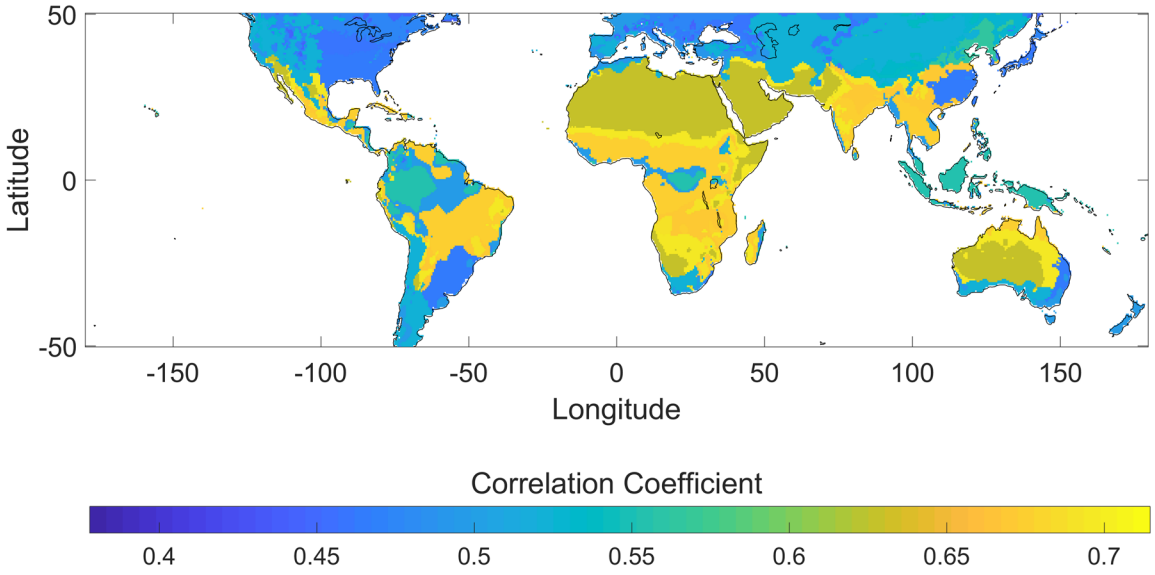

Figure 8. Average correlation coefficients by Koppen-Geiger climate classification regimes.

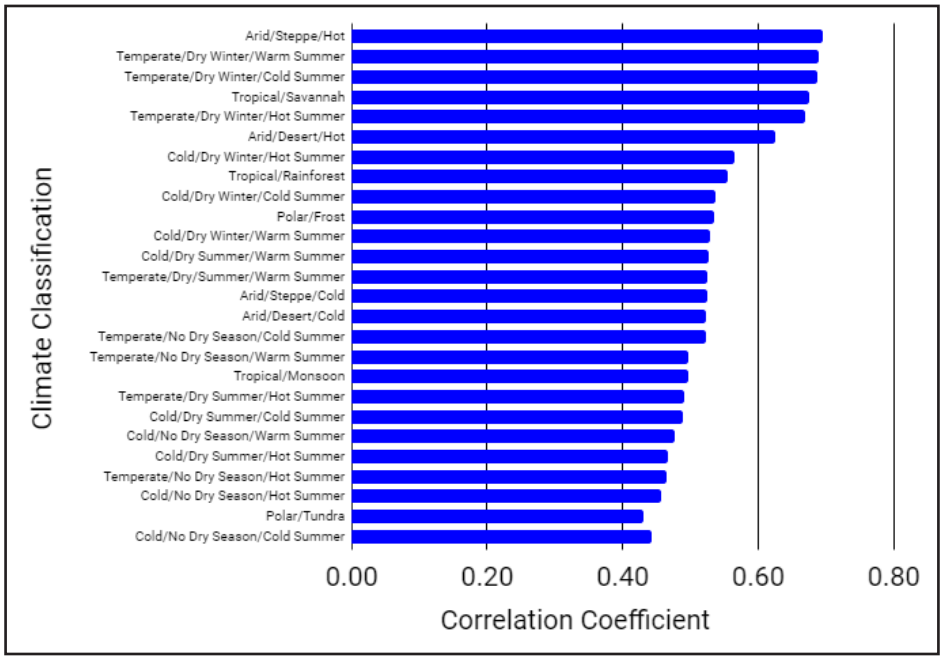

Figure 9. Bar plot of average correlation coefficient by Koppen-Geiger climate classification regimes.

between them tends to be inverse in major river basins, plausibly due to two physical processes, including hydraulic redistribution by tropical trees (Harper et al. 2010; Yan and Dickinson 2014), as well as river transport and expansion caused by upstream precipitation (Conway 2000, 2005).

Additionally, this study served as an informal validation of SMAP soil moisture data using TMPA precipitation data. TMPA precipitation helped validate SMAP soil moisture because in most locations on the globe, when moderate rain occurred soil moisture also increased, as indicated by predominantly positive correlations. The presence of negative correlations in this study may also add to the validity of SMAP data rather than taking away from it. For example, logically, irrigated regions should, at times, show an opposite relationship between soil moisture and

precipitation. In addition, certain rainforests show an opposite relationship between soil moisture and precipitation, due to recent findings that rainforest tree roots transport groundwater to the top soil in order to survive dry seasons (Harper et al. 2010). Moreover, this study of incorporating landcover and climate regimes in our analyses further supports SMAP's credibility based on the different types of landcover and climate regimes. For example, savanna landcover and arid/steppe/hot climates experience a strong correlation between TRMM and SMAP because both precipitation and soil moisture are truly low in these environments, and both satellites were able to reflect those conditions.

Acknowledgments

This work was supported by the [NASA Minority University Research and Education Project (MUREP) Institutional Research Opportunity] under Grant [NNX15AQ06A]. The authors would like to thank the reviewers and editors for their constructive comments and suggestions during the review process of this article.

Author Bio and Contact Information

Robin Sehler is a recent graduate of California State University, Los Angeles. She holds a Master's Degree in Environmental Studies, with an emphasis in Geospatial Information Systems, and a Bachelor's Degree in Geology. Robin has focused most of her research on NASA satellite data, and has studied various topics such as the subsurface of planet Venus, global SST, California levy seepage detection, Mississippi River discharge, and, more recently, the global correlation between precipitation and soil moisture data. Robin submitted Ph.D. applications this winter, and hopes to continue studying soil moisture, with a closer look at plant functioning. She may be contacted at robin.sehler@gmail.com or 13210 Winterberry Way, Princeton, NJ 08540.

Jingjing Li (corresponding author) is an Assistant Professor of Hydrology at California State University, Los Angeles. She received her Ph.D. in Civil Engineering from University of California, Irvine. Her research interests include remote sensing, precipitation error analysis, GIS-based modeling of watershed-scale processes, hydrologic modeling, and image processing. Her research has been published in journals such as Water Resources Research, Journal of Hydrometeorology, and International Journal of Remote Sensing. She has presented her work at conferences and research centers, including NASA JPL, NASA GSFC, and AGU. She is Co-I of a $5-million NASA grant "Data Intensive Research and Education Center for STEM." She may be contacted at jli104@calstatela.edu or 5151 State University Dr. (KH-C4067), Los Angeles, CA 90032.

JT Reager is a Research Scientist in the Surface Hydrology group at Jet Propulsion Laboratory. He received his Ph.D. in Earth System Science from University of California, Irvine. He studies the Earth's water cycle with a particular focus on hydrologic extremes, sea level rise, and water resources. He is awardee of NASA Early Career Achievement Medal for contributions to understanding hydrologic extreme events. He is the PI and Co-I on more than ten research projects funded by NASA and JPL. His research has published in high impact journals, such as Science, Nature Climate Change, and Journal of Hydrology. He may be contacted at John.Reager@jpl.nasa.gov or 4800 Oak Grove Drive (M/S 300-323), Pasadena, CA 91109.

Hengchun Ye is a Professor and Associate Dean of the College of Natural and Social Sciences at the California State University, Los Angeles. She received a Ph.D in Climatology from the University of Delaware. Her research expertise is in climate variability and change that are reflected on changing precipitation characteristics over high latitude regions. Dr. Ye has published over 60 peer-review manuscripts, many in high impact journals and as the first author. Dr. Ye also has a passion in education and research training for under-represented students in STEM and has secured over $6.5 million in grants supporting these efforts. She may be contacted at hye2@calstatela.edu or 5151 State University Dr. (ASC B223), Los Angeles, CA 90032.

References

AghaKouchak, A., A. Behrangi, S. Sorooshian, K. Hsu, and E. Amitai. 2011. Evaluation of satellite-retrieved extreme precipitation rates across the central United States. *Journal of Geophysical Research* 116(D2).

Boé, J. 2013. Modulation of soil moisture–precipitation interactions over France by large scale circulation. *Climate Dynamics* 40(3-4): 875-892.

Brodzik, M.J., B. Billingsley, T. Haran, B. Raup, and M.H. Savoie. 2012. EASE-Grid 2.0: Incremental but significant improvements for Earth-gridded data sets. *ISPRS International Journal of Geo-Information* 1(1): 32-45.

Channan, S., K. Collins, and W.R. Emanuel. 2014. Global mosaics of the standard MODIS land cover type data. University of Maryland and the Pacific

Northwest National Laboratory, College Park, Maryland, USA.

Conway, D. 2000. The climate and hydrology of the Upper Blue Nile River. *The Geographical Journal* 166(1): 49-62. Available at: https://doi.org/10.1111/j.1475-4959.2000.tb00006.x. Accessed August 27, 2019.

Conway, D. 2005. From headwater tributaries to international river: Observing and adapting to climate variability and change in the Nile basin. *Global Environmental Change* 15(2): 99-114. Available at: https://doi.org/10.1016/j.gloenvcha.2005.01.003. Accessed August 27, 2019.

Cook, B.I., G.B. Bonan, and S. Levi. 2006. Soil moisture feedbacks to precipitation in southern Africa. *Journal of Climate* 19: 4198-4206.

Cui, C., J. Xu, J. Zeng, K-S. Chen, X. Bai, H. Lu, Q. Chen, and T. Zhao. 2018. Soil moisture mapping from satellites: An intercomparison of SMAP, SMOS, FY3B, AMSR2, and ESA CCI over two dense network regions at different spatial scales. *Remote Sensing* 10: 33. Available at: https://doi.org/10.3390/rs10010033. Accessed August 27, 2019.

Das, N.N., D. Entekhabi, A. Colliander, F. Chen, W. Crow, T. Jackson, and S. Yueh. 2015. *Soil Moisture Active Passive (SMAP) Project Calibration and Validation for the L2/3_SM_AP Beta-Release Data Products*. Available at: https://nsidc.org/sites/nsidc.org/files/technical-references/SMAP-AP_Assessment_Report_Final.pdf. Accessed August 27, 2019.

Eltahir, E.A.B. 1998. A soil moisture–rainfall feedback mechanism: 1. Theory and observations. *Water Resources Research* 34(4): 765-776.

Entekhabi, D., E.G. Njoku, P.E. O'Neill, K.H. Kellogg, W.T. Crow, W.N. Edelstein, J.K. Entin, S.D. Goodman, T.J. Jackson, J. Johnson, … and J. Van Zyl. 2010. The soil moisture active passive (SMAP) mission. *Proceedings of the IEEE* 98(5): 704-716.

Entekhabi, D., S. Yueh, P. O'Neill, K. Kellogg, A. Allen, R. Bindlish, ... and W.T. Crow. 2014. SMAP Handbook: Mapping Soil Moisture and Freeze/Thaw from Space. NASA, Jet Propulsion Laboratory, Pasadena, CA. Available at: https://soilsensor.com/wp-content/uploads/SMAP_Handbook_FINAL_1_JULY_2014_Web.pdf. Accessed August 27, 2019.

Famiglietti, J.S. and M. Rodell. 2013. Water in the balance. *Science* 340(6138): 1300-1301.

Feng, H. and M. Zhang. 2015. Global land moisture trends: Drier in dry and wetter in wet over land. *Scientific Reports* 5: 18018. DOI: 10.1038/srep18018.

Findell, K.L. and E.A.B. Eltahir. 1997. An analysis of the soil moisture-rainfall feedback, based on direct observations from Illinois. *Water Resources Research* 33(4): 725-735.

Fisher, R.A. 1985. *Statistical Methods for Research Workers*, 13th Ed. Hafner, New York, NY.

Ford, T.W., A.D. Rapp, and S.M. Quiring. 2015a. Does afternoon precipitation occur preferentially over dry or wet soils in Oklahoma? *Journal of Hydrometeorology* 16(2): 874-888.

Ford, T.W., A.D. Rapp, S.M. Quiring, and J. Blake. 2015b. Soil moisture–precipitation coupling: Observations from the Oklahoma Mesonet and underlying physical mechanisms. *Hydrology and Earth System Science* 19: 3617-3631.

Greve, P., B. Orlowsky, B. Mueller, J. Sheffield, M. Reichstein, and S.I. Seneviratne. 2014. Global assessment of trends in wetting and drying over land. *Nature Geoscience* 7: 716-721.

Guillod, B.P., B. Orlowsky, D.G. Miralles, A.J. Teuling, and S.I. Seneviratne. 2015. Reconciling spatial and temporal soil moisture effects on afternoon rainfall. *Nature Communications* 6: 6443.

Harper, A.B., A.S. Denning, I.T. Baker, M.D. Branson, L. Prihodko, and D.A. Randall. 2010. Role of deep soil moisture in modulating climate in the Amazon Rainforest. *Geophysical Research Letters* 37: 1-6. Available at: https://doi.org/10.1029/2009GL042302. Accessed August 27, 2019.

Huffman, G.J., R.F. Adler, D.T. Bolvin, G. Gu, E.J. Nelkin, K.P. Bowman, Y. Hong, E.F. Stocker, and D.B. Wolff. 2007. The TRMM Multisatellite Precipitation Analysis (TMPA): Quasi-global, multiyear, combined-sensor precipitation estimates at fine scales. *Journal of Hydrometeorology* 8: 38-55.

Huffman, G.J. and D.T. Bolvin. 2015. TRMM and Other Data Precipitation Data Set Documentation. Available at: https://pmm.nasa.gov/sites/default/files/document_files/3B42_3B43_doc_V7.pdf. Accessed August 27, 2019.

James, A.L. and N.T. Roulet. 2009. Antecedent moisture conditions and catchment morphology as controls on spatial patterns of runoff generation in small forest catchments. *Journal of Hydrology* 377: 351-366.

Kerr, Y., E. Jacquette, A. Al Bitar, F. Cabot, A. Mialon, P. Richaume, and J. Wigneron. 2013. CATDS SMOS L3 Soil Moisture Retrieval Processor. Algorithm Theoretical Baseline Document (ATBD). SO-TN-CBSA-GS-0029. Available at: http://www.cesbio.ups-tlse.fr/SMOS_blog/wp-content/uploads/2013/08/ATBD_L3_rev2_draft.pdf. Accessed August 27, 2019.

Koster, R.D., P.A. Dirmeyer, Z. Guo, G. Bonan, E. Chan, P. Cox, C.T. Gordon, S. Kanae, E. Kowalczyk, D. Lawrence, … and T. Yamada. 2004. Regions of strong coupling between soil moisture and precipitation. *Science* 305: 1138-1140.

Liang, L., S. Peng, J. Sun, L. Chen, and Y. Cao. 2010. Estimation of annual potential evapotranspiration at regional scale based on the effect of moisture on soil respiration. *Ecological Modeling* 221: 2668-2674.

Ma, C., X. Li, L.Wei, and W. Wang. 2017. Multi-scale validation of SMAP soil moisture products over cold and arid regions in Northwestern China using distributed ground observation data. *Remote Sensing* 9(4): 327. Available at: https://doi.org/10.3390/rs9040327. Accessed August 27, 2019.

McCabe, G.J. and D.M. Wolock. 2013. Temporal and spatial variability of global water balance. *Climatic Change* 120: 375-387.

McColl, K.A., S.H. Alemohammad, R. Akbar, A.G. Konings, S.Yueh, and D. Entekhabi. 2017. The global distribution and dynamics of surface soil moisture. *Nature Geoscience* 10: 100-104. Available at: https://doi.org/10.1038/ngeo2868. Accessed August 27, 2019.

O'Neill, P.E., S. Chan, E.G. Njoku, T. Jackson, and R. Bindlish. 2016. SMAP L3 Radiometer Global Daily 36 km EASE-Grid Soil Moisture, Version 4. [L3V4]. Boulder, Colorado, USA. NASA National Snow and Ice Data Center Distributed Active Archive Center. Available at: http://dx.doi.org/10.5067/OBBHQ5W22HME. Accessed August 27, 2019.

O'Neill, P.E., S. Chan, E.G. Njoku, T. Jackson, and R. Bindlish. 2018. Algorithm Theoretical Basis Document Level 2 & 3 Soil Moisture (Passive) Data Products. Revision D. SMAP Project, JPL D-66480, Jet Propulsion Laboratory, Pasadena, CA.

Pan B., K. Hsu, A. AghaKouchak, S. Sorooshian, and W. Higgins. 2019. Precipitation prediction skill for the West Coast United States: From short to extended range. *Journal of Climate* 32(1): 161-182. DOI: 10.1175/JCLI-D-18-0355.1.

Peel, M.C., B.L. Finlayson, and T.A. McMahon. 2007. Updated world map of the Köppen-Geiger climate classification. *Hydrology and Earth System Sciences Discussions* 11(5): 1633-1644.

Sapiano, M.R.P. and P.A. Arkin. 2009. An intercomparison and validation of high-resolution satellite precipitation estimates with 3-hourly gauge data. *Journal of Hydrometeorology* 10: 149-166.

Wentz, F.J., T. Meissner, C. Gentemann, and M. Brewer. 2014. Remote Sensing Systems AQUA AMSR-E 3-Day Environmental Suite on 0.25 Deg Grid, Version 7.0. Remote Sensing Systems, Santa Rosa, CA. Available at: http://www.remss.com/missions/amsr/. Accessed August 27, 2019.

Yan, B. and R.E. Dickinson. 2014. Modeling hydraulic redistribution and ecosystem response to droughts over the Amazon Basin using Community Land Model 4.0 (CLM4). *Journal of Geophysical Research: Biogeosciences* 119: 2130-2143. DOI: 10.1002/2014JG002694.

Yang, L., G. Sun, L. Zhi, and J. Zhao. 2018. Negative soil moisture-precipitation feedback in dry and wet regions. *Scientific Reports* 8(1).

Zhang, X., T. Zhang, P. Zhou, Y. Shao, and S. Gao. 2017. Validation analysis of SMAP and AMSR2 soil moisture products over the United States using ground-based measurements. *Remote Sensing* 9: 104. Available at: https://doi.org/10.3390/rs9020104. Accessed August 27, 2019.

Zheng, X. and E.A.B. Eltahir. 1998. A soil moisture–rainfall feedback mechanism: 2. Numerical experiments. *Water Resources Research* 34: 777-785.